Observation of localized flat-band states in Kagome photonic lattices

Yuanyuan Zong,[1,3] Shiqiang Xia,[1,3] Liqin Tang,[1,*] Daohong Song,[1] Yi Hu,[1] Yumiao Pei,[1] Jing Su,[1] Yigang Li,[1] and Zhigang Chen[1,2]

[1]*The MOE Key Laboratory of Weak-Light Nonlinear Photonics, TEDA Applied Physics Institute and School of Physics, Nankai University, Tianjin 300457, China*
[2]*Department of Physics and Astronomy, San Francisco State University, San Francisco, California 94132, USA*
[3]*These authors contributed equally to this work*
[*]*tanya@nankai.edu.cn*

Abstract: We report the first experimental demonstration of localized flat-band states in optically induced Kagome photonic lattices. Such lattices exhibit a unique band structure with the lowest band being completely flat (diffractionless) in the tight-binding approximation. By taking the advantage of linear superposition of the flat-band eigenmodes of the Kagome lattices, we demonstrate a high-fidelity transmission of complex patterns in such two-dimensional pyrochlore-like photonic structures. Our numerical simulations find good agreement with experimental observations, upholding the belief that flat-band lattices can support distortion-free image transmission.

OCIS codes: (130.0130) Integrated optics; (130.2790) Guided waves; (230.0230) Optical devices; (230.7370) Waveguides; (230.3120) Integrated optics devices.

References and links

1. N. K. Efremidis, S. Sears, D. N. Christodoulides, J. W. Fleischer, and M. Segev, "Discrete solitons in photorefractive optically induced photonic lattices," Nature (London) **66**, 046602 (2002).
2. J. W. Fleischer, M. Segev, N. K. Efremidis, and D. N. Christodoulides, "Observation of two-dimensional discrete solitons in optically induced nonlinear photonic lattices," Nature (London) **422**, 147–150 (2003).
3. F. Lederer, G. I. Stegeman, D. N. Christodoulides, G. Assanto, M. Segev, and Y. Silberberg, "Discrete solitons in optics," Phys. Rep. **463**, 1–126 (2008).
4. Z. Chen, M. Segev, and D.N. Christodoulides, "Optical spatial solitons: historical overview and recent advances," Rep. Prog. Phys. **75**, 086401 (2012).
5. S. Longhi, M. Marangoni, M. Lobino, R. Ramponi, P. Laporta, E. Cianci, and V. Foglietti, "Observation of dynamic localization in periodically curved waveguide arrays," Phys. Rev. Lett. **96** 243901 (2006).
6. T. Schwartz, G. Bartal, S. Fishman, and M. Segev, "Transport and Anderson localization in disordered two-dimensional photonic lattices," Nature (London) **446**, 52 (2007).
7. A. Szameit, F. Dreisow, M. Heinrich, T. Pertsch, S. Nolte, A. Tünnermann, E. Suran, F. Louradour, A. Barthélémy, and S. Longhi, "Image reconstruction in segmented femtosecond laser-written waveguide arrays," Appl. Phys. Lett. **93**, 181109 (2008).
8. A. Szameit, Y. V. Kartashov, F. Dreisow, M. Heinrich, T. Pertsch, S. Nolte, A. Tünnermann, V. A. Vysloukh, F. Lederer, and L. Torner, "Inhibition of light tunneling in waveguide arrays," Phys. Rev. Lett. **102**(15), 153901 (2009).
9. P. Zhang, N. K. Efremidis, A. Miller, Y. Hu, and Z. Chen, "Observation of coherent destruction of tunneling and unusual beam dynamics due to negative coupling in three-dimensional photonic lattices," Opt. Lett. **35**(19), 3252–3254 (2010).
10. J. Yang, P. Zhang, M. Yoshihara, Y. Hu, and Z. Chen, "Image transmission using stable solitons of arbitrary shapes in photonic lattices," Opt. Lett. **36**, 772 (2011).

#259832 Received 23 Feb 2016; revised 6 Apr 2016; accepted 11 Apr 2016; published 14 Apr 2016

11. R. Keil, Y. Lahini, Y. Shechtman, M. Heinrich, R. Pugatch, F. Dreisow, A. Tünnermann, S. Nolte, and A. Szameit, "Perfect imaging through a disordered waveguide lattice," Appl. Phys. Lett. **37**, 809 (2012).
12. H. Aoki, M. Ando and H.Matsumura, "Hofstadter butterflies for flat bands," Phys. Rev. B **54**, R17296 (1996).
13. R. A. Vicencio, C. Cantillano, L. Morales-Inostroza, B. Real, C. Mejia-Cortes, S. Weimann, A. Szameit, and M. I. Molina, "Observation of localized states in Lieb photonic lattices," Phys. Rev. Lett. **114**, 245503 (2015).
14. S. Mukherjee, A. Spracklen, D. Choudhury, N. Goldman, P. Ohberg, E. Andersson and R. R. Thomson, "Observation of a localized flat-band state in a photonic Lieb lattice," Phys. Rev. Lett. **114**, 245504 (2015).
15. S. Xia, Y. Hu, D. Song, Y. Zong, L. Tang, and Z. Chen, "Demonstration of flat-band image transmission in optically induced Lieb photonic lattices," Opt. Lett. **41(7)**, 1435–1438 (2016).
16. J. L. Atwood, "Kagome lattice: a molecular toolkit for magnetism," Nat. Mater. **1**, 91 (2002).
17. D. L. Bergman, C. Wu, and L. Balents, "Band touching from real-space topology in frustrated hopping models," Phys. Rev. B **78**, 125104 (2008).
18. B. Moulton, J. Lu, R. Hajndl, S. Hariharan, and M. J. Zaworotko, "Crystal engineering of a nanoscale kagome lattice," Angew. Chem. Int. Ed. Engl. **41**, 2821–2824 (2002).
19. Y. Nakata, T. Okada, T. Nakanishi, and M. Kitano, "Observation of flat band for terahertz spoof plasmon in metallic kagome lattice," Phys. Rev. B **85**, 205128 (2012).
20. S. Endo, T. Oka, and H. Aoki, "Tight-binding photonic bands in metallophotonic waveguide networks and flat bands in kagome lattices," Phys. Rev. B **81**, 113104 (2010).
21. H. Takeda, T. Takashima, and K. Yoshino, "Flat photonic bands in two-dimensional photonic crystals with kagome lattices," J. Phys.: Condens. Matter **16**, 6317 (2004).
22. M. Boguslawski, P. Rose, and C. Denz, "Nondiffracting kagome lattice," Appl. Phys. Lett. **98**, 061111 (2011).
23. Y. Gao, D. Song, S. Chu, and Z. Chen, "Artificial graphene and related photonic lattices generated with a simple method," *IEEE Photonics J.*, **6**, 2201806 (2014).
24. R. A. Vicencio and C. Meja-Corts, "Diffraction-free image transmission in kagome photonic lattices," J. Opt. **16**, 015706 (2014).
25. O. Peleg, G. Bartal, B. Freedman, O. Manela, M. Segev, and D. N. Christodoulides, "Conical diffraction and gap solitons in honeycomb photonic lattices," Phys. Rev. Lett. **98**, 103901 (2007).
26. D. Song, V. Paltoglou, S. Liu, Y. Zhu, D. Gallardo, L. Tang, J. Xu, M. Ablowitz, N. K. Efremidis, and Z. Chen, "Unveiling pseudospin and angular momentum in photonic graphene," Nat. Commun. **6** 6272 (2015).
27. H. Martin, E. D. Eugenieva, Z. Chen, and D. N. Christodoulides, "Discrete solitons and soliton-induced dislocations in partially coherent photonic lattices," Phys. Rev. Lett. **92**, 123902 (2004).
28. A. Kelberer, M. Boguslawski, P. Rose, and C. Denz, " Embedding defect sites into hexagonal nondiffracting wave fields," Opt. Lett. **37**, 5009–5011 (2012).
29. R. A. Vicencio and M. Johansson, "Discrete flat-band solitons in the kagome lattice," Phys. Rev. A **87**, 061803(R) (2013).
30. G. Chern and A. Saxena, "PT-symmetric phase in kagome photonic lattices," Opt. Lett. **40**(24), 5806–5809 (2015).
31. S. Mukherjee and R. R. Thomson, "Observation of localized flat-band modes in a quasi-one-dimensional photonic rhombic lattice," Opt. Lett. **40**, 5443–5446 (2015).

1. Introduction

Nondestructive transmission of optical information has always been a challenging subject of research. Over the past several years, evanescently coupled waveguide arrays, or better known as photonic lattices, have provided an extremely effective platform for studying many intriguing fundamental phenomena ranging from discrete solitons to dynamical localization and Anderson localization in disordered lattices [1–6]. They have also been explored for applications such as image transmission in a variety of optical settings [7–11]. In particular, recent developments in the so-called flat-band [12] lattices have opened up new avenues for manipulation of light and controlled image transmission. For instance, Lieb photonic lattices were realized via the femtosecond laser-writing technique as well as the optical induction technique, allowing for direct observations of diffractionless flat-band states [13–15]. In these recent experimental demonstrations, the Lieb photonic lattices remain perfectly periodic without any modulation, yet they are able to support localized states due to the principle of phase cancellation which is a common feature of flat-band eigenstates [12].

A Kagome lattice is a triangular depleted lattice that is essentially a two-dimensional (2D) counterpart of the "pyrochlore" structure, which has been historically studied as a model for

#259832 Received 23 Feb 2016; revised 6 Apr 2016; accepted 11 Apr 2016; published 14 Apr 2016

geometrically frustrated magnetism and for presenting the flat bands [16, 17]. For decades in condensed matter physics, Kagome lattices have been the subject mainly for theoretical study due to their intriguing properties associated with spin frustration. But technology advancement has turned them from theory into reality, including for example the realization of nanoscale Kagome lattices by self-assembling atoms and molecules [18] and metallic Kagome lattices by novel design and fabrication of metamaterials [19]. Several schemes were theoretically proposed to create flat bands in the 2D Kagome lattice, utilizing metallo-photonic waveguides [20] or using photonic crystal structures [21]. In optics, photonic Kagome lattices have also been established using the technique of optical induction [22, 23]. In fact, recently it has been proposed theoretically that the flat-band system in a Kagome photonic lattice could be used for diffraction-free image transmission [24]. However, up to now, undistorted propagation of flat-band states in Kagome photonic lattices has not been accomplished experimentally to the best of our knowledge.

In this paper, we report the first experimental demonstration of a localized flat-band state in Kagome photonic lattices. The Kagome lattices are "fabricated" in a bulk self-focusing nonlinear crystal by a simple yet effective optical induction technique. Such induction technique is based on optical Fourier transformation through an amplitude mask superimposed with a phase mask, without the need of using a spatial light modulator (SLM) for engineering the lattice-inducing beam. We show that optically induced Kagome lattices offer a convenient platform for probing the flat-band states. Furthermore, we realize a high-fidelity bound-state transmission in such 2D pyrochlore-like photonic structures by judiciously exciting a superposition of flat-band eigenmodes of the Kagome lattices. Comparing with our previous work on Lieb lattices [15], which are more feasible for square or L-shaped image transmission, in Kagome lattices the flat band is in the "ground-state", and their localized mode structures are more suitable for ring or necklace-shaped image transmission.

2. Theoretical model and linear spectrum

The linear propagation of a light beam in photonic lattices is well described by the following Schrödinger-like equation under paraxial approximation [1–3]:

$$i\frac{\partial \psi(x,y,z)}{\partial z} = -\frac{1}{2k_1}\bigtriangledown^2 \psi(x,y,z) - k_0 \Delta n(x,y)\psi(x,y,z) \tag{1}$$

where (x,y) are the transverse coordinates, z represents the longitudinal propagation direction, and ψ corresponds the electric field envelop of the probe beam. $\bigtriangledown^2$ is the 2D transverse Laplacian operator. n_0 is the refractive index of the nonlinear medium, $k_0 = 2\pi/\lambda_0$ is the wave number in the vacuum, and $k_1 = n_0 k_0$. The refractive index change is $\Delta n(x,y) = n_0^3 \gamma_{33} E_0 / [2(1+I_l)]$, which represents the refractive index changes corresponding to the 2D Kagome photonic lattices. I_l is the Kagome intensity pattern, $n_0 = 2.35$, the electro-optic coefficient $\gamma_{33} = 280$ pm/V, and the bias field $E_0 = 1$ kV/cm.

Assuming that only the hopping between the nearest-neighbor lattice sites is considered, we can use the tight-binding model to solve Eq. (1). Here we consider the 2D Kagome photonic lattice shown in Fig. 1(a) as the index changes (potential) in Eq. (1). Figure 1(b) shows a 3D plot of the band structure in k-space. In this case, the linear spectrum exhibits three bands: two dispersive and one nondispersive (flat) band in a unitary cell of the Kagome lattice [dashed triangle of Fig. 1(a)]. Similar to honeycomb lattices [25, 26], the curved bands are featured by the linear dispersion relation in the vicinity of Dirac points (six K points), where the Dirac cones from the upper and lower bands are integrated. The bottom of the lower band touches the third (flat) band at Γ point of the first Brillouin zone (BZ). As seen from the Fig. 1(b), the third band is a completely degenerated flat band. The presence of the flat band which comes from local in-

#259832 Received 23 Feb 2016; revised 6 Apr 2016; accepted 11 Apr 2016; published 14 Apr 2016

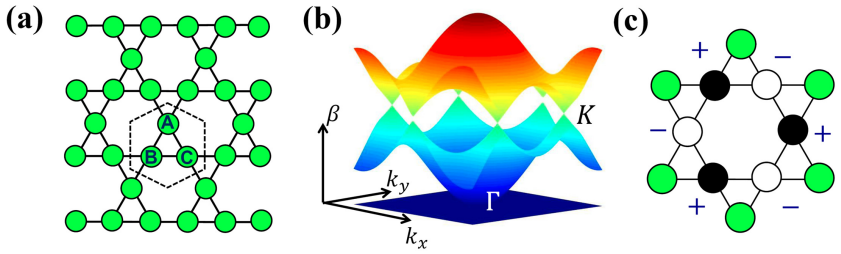

Fig. 1. (a) A schematic diagram of 2D Kagome lattice structure with each unit cell consisting of three lattice sites marked as A, B, C. (b) Numerically calculated band structure under the tight-binding approximation, showing the first three bands with the flat band at the bottom. (c) A fundamental (ring) mode as the flat-band localized degenerate eignstate is denoted by black and white circles, all possessing equal intensity but alternating opposite phases.

terference effect is the significant feature in this band structure. The localized eigenmodes in the flat-band are called "ring" modes with equal amplitudes but alternating opposite phases [24], which are marked as black and white circles [see the Fig. 1(c)]. Different from modes in normal Bloch bands, the flat-band linear wave functions (flat-band states) are not completely extended due to the destructive interference. The purpose of this paper is to experimentally demonstrate the predicted localized flat-band modes in Kagome photonic lattices, and to explore the possibility to use superposition of these modes for distortion-free image transmission through bulk media.

3. Optical induction of Kagome photonic lattices

First, we fabricate the Kagome photonic lattices using the well-established optical induction technique [1, 2]. The experimental setup used for lattice induction and excitation of the flat-band states is shown in Fig. 2(a). A laser beam operating at 532nm is divided into three paths (as labeled in the figure): the first path is the lattice-forming beam, the second path is the probe beam, and the third path provides a reference beam for interference measurement as needed. Lattice-forming beam [Fig. 2(a), the line of the red arrow 1] is ordinarily polarized and is partially spatially incoherent after passing through a rotating diffuser. To generate the Kagome lattices intensity pattern, this partially incoherent beam is further modulated by a specially designed amplitude mask and a spectral filter (phase mask 1) positioned at the Fourier plane [23]. The phase mask 1 (PM1) is used to spatially filter the light and modulate the phase of spatial frequency spectrum in the front focal plane of the transform lens. The PM1 consists of six holes, three of them covered with tilted glass plates to adjust the relative phase. The diameter of each hole is 0.8 mm and the spacing between adjacent holes is 4.0 mm. When the phase difference of the adjacent spatial frequency spectrum is $2\pi/3$, the Kagome lattice is established. This combined modulation leads to a Kagome intensity pattern on the front facet of the photorefractive crystal (SBN: 5 mm$\times$10 mm$\times$5 mm), which leads to a Kagome index lattice when the crystal is biased by an electric field that provides a self-focusing nonlinearity. The technique using partially incoherent light beam for optical induction of photonic lattices is well established in literature, as used for earlier experiments on discrete solitons [27] and for recent demonstrations of photonic graphene lattices and Kagome lattices [23, 26]. Thus, in this work, we use the technique to create a Kagome lattice which can remain stable and nearly invariant along the direction of propagation throughout the nonlinear crystal for testing the flat-band states, but our focus is not on lattice induction.

#259832 Received 23 Feb 2016; revised 6 Apr 2016; accepted 11 Apr 2016; published 14 Apr 2016

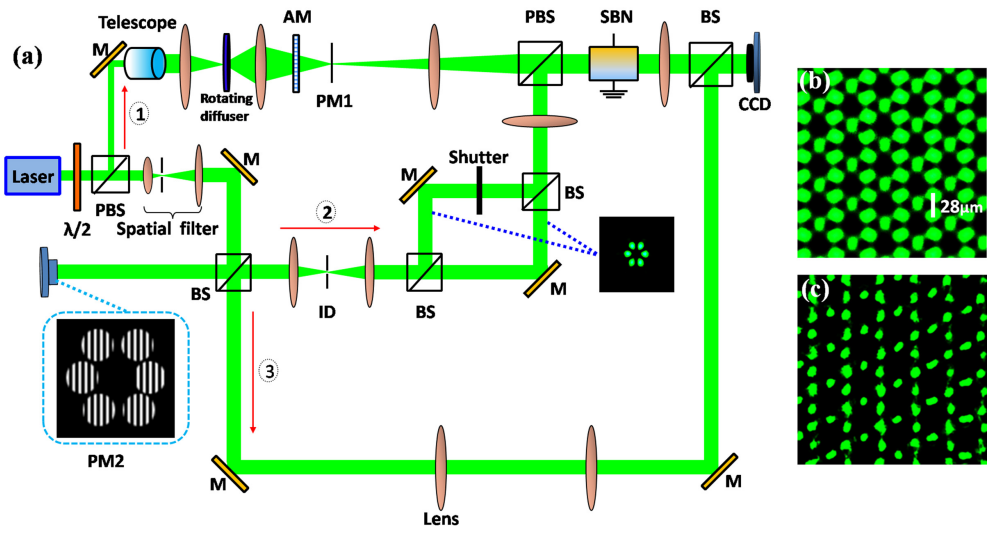

Fig. 2. (a) Experimental setup: (P)BS: (polarizing) beam splitter; ID: iris diaphragm; M: mirror; SBN: strontium barium niobate; SLM: phase-only spatial light modulator; AM: amplitude mask; PM1 (phase mask 1): phase modulation to lattice-forming beam at Fourier plane; PM2 (phase mask 2): phase modulation to probe beam encoded onto SLM. Red arrows 1, 2, 3 show, respectively, the lattice-forming beam, the probe beam, and the interfering beam for measuring the output phase structure. (b) Experimentally established Kagome lattice with lattice spacing of 28 μm. (c) Output of the guided intensity pattern of a quasi-plane wave by the corresponding Kagome structured waveguide arrays.

In the second path (the line of the red arrow 2), the probe beam is extraordinarily polarized. In order to excite a flat-band state, we use a phase-only spatial light modulator (SLM) to modulate the phase of the probe beam. We simultaneously encode the amplitude and the phase information onto SLM by designing a hologram (phase mask 2) consisting several phase gratings arranged in a hexagonal structure as shown in the bottom-left insert of Fig. 2(a). When the hologram is encoded onto the SLM, a broad extraordinarily polarized quasi-plane wave is sent to the SLM, and then first order of the diffracted light is filtered through an adjustable diaphragm. With this method, we can obtain a probe beam with a necklace-like intensity pattern with a desired phase structure as needed for the "ring" mode shown in Fig. 1(c). After modulating by the SLM, the probe beam is divided into two parts by a Mach-Zehnder interferometer with a mechanical shutter inserted in one arm. When the shutter is closed, the probe beam only excites one flat-band eigenmode (i.e, a localized "ring" mode). However, when the shutter is open, the two outputs from the interferometer can be superimposed to generate a complex pattern (an elongated necklace) to excite two "ring" modes as a flat-band bound state. The size of each intensity spot of the probe beam at input is controlled by the imaging lens, and the spacing between adjacent spots is controlled via adjusting the phase gratings. Meanwhile, the phase structure of the probe beam can be controlled via fine-tuning the relative localizations of the six gratings. For example, when the stripes of the nearest neighboring gratings are staggered arranged as shown in PM2, we can get a probe beam with an out-of phase structure, whereas unstaggered grating arrangement leads to in-phase condition of the probe beam. In addition, the input/output intensity profiles of the probe beams and the Kagome lattices are monitored with a CCD camera. To examine the phase structure of different profiles, we use the third path beam as a tilted reference quasi-plane wave to obtain interferograms.

#259832 Received 23 Feb 2016; revised 6 Apr 2016; accepted 11 Apr 2016; published 14 Apr 2016

The crystal used in our experiments is a 10-mm long SBN: 60 under a positive bias field of 1.6 KV/cm. The orientation of the crystal's symmetry c-axis is at horizontal direction, and the applied electric field is along the crystalline c-axis. Typical experimental results for an optically induced Kagome lattice of 28 μm are shown in Figs. 2(b) and 2(c). Figure 2(b) depicts the output intensity distribution for the induced Kagome lattice at the back face of the crystal. In order to test the Kagome structured waveguide, a broad uniform beam (quasi-plane wave) is used as a probe to the lattice, and its output after propagating through the lattice is shown in Fig. 2(c), exhibiting clearly a Kagome structure due to linear guidance by the lattice-induced waveguide arrays. In our experiments, the ordinarily-polarized lattice-inducing beam would experience only weak nonlinear index change, so the anisotropic photorefractive nonlinearity does not play a significant role. On the other hand, the diffraction along the two orthogonal principal axes is slightly different due to inherent orientation anisotropy in the Kagome lattices. So we make the direction with slightly stronger diffraction along the crystalline c-axis (i.e., the direction with stronger nonlinearity) in our experiments. Using this method, our induced Kagome lattices are pretty uniform in both directions and are not afflicted by the anisotropic nonlinearity, as seen in Fig. 2(c) for the output intensity distribution of the guided wave pattern.

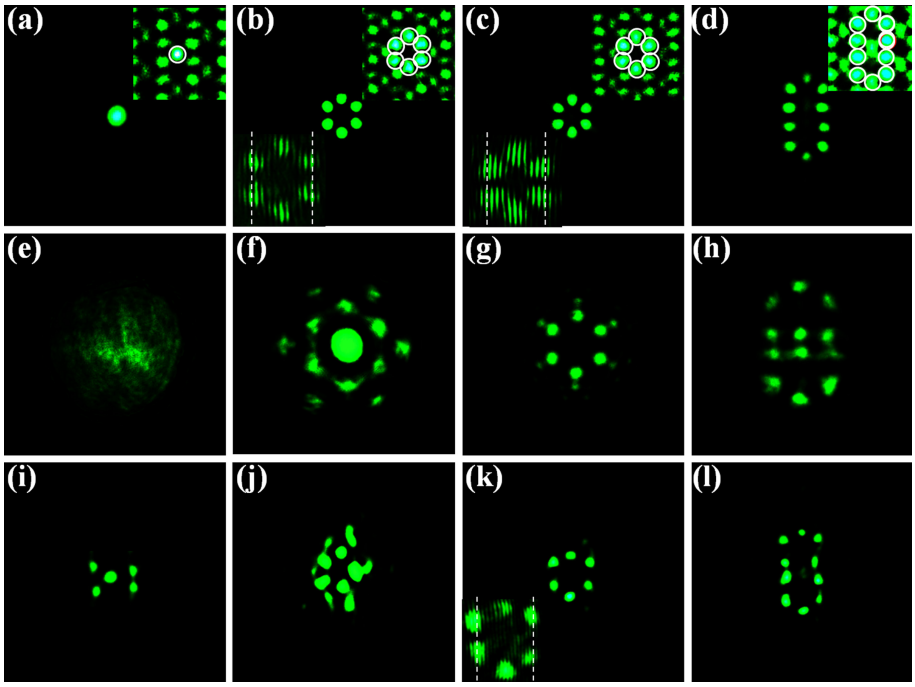

Fig. 3. Experimental demonstration of localized flat-band states and their superposition propagating through the Kagome lattice. From left to right, shown are for probing with a single Gaussian beam, six-spot (necklace) beam with equal phase, six-spot beam with opposite phase (as a flat-band state), and an elongated necklace beam (as superposition of ring modes). (a)–(d) Input beam patterns, (e)–(h) linear output patterns without the Kagome lattice, and (i)–(l) linear output patterns exiting the lattice. Upper insets show the combined input intensity patterns when the probe beam is launched into the lattice, and lower insets (zoomed in) show the interferograms of (b) and (c) with a tilted quasi-plane wave to show the input phase structure.

#259832 Received 23 Feb 2016; revised 6 Apr 2016; accepted 11 Apr 2016; published 14 Apr 2016

4. Demonstration of localized flat-band states in Kagome photonic lattices

Next, we demonstrate experimentally non-diffracting propagation of flat-band modes and their superposition in the Kagome lattice. Typical experimental results are shown in Fig. 3. The first row shows the intensity distribution of the probe beams under different settings [Figs. 3(a)–3(d)]. For comparison, the output intensity distributions for different input as probe all display linear diffraction without the induced lattice [Figs. 3(e)–3(h)]. When the desired input modes are launched into the lattice, localized output is observed after propagating 10 mm through the lattice. The localization is very sensitive to the modes excited at the input [Figs. 3(i)–3(l)], in contradistinction to that from disorder-induced localization. As expected, a single Gaussian beam experiences discrete diffraction in the lattice [Fig. 3(i)]. A six-spot necklace pattern cannot be localized if they are all in phase [Fig. 3(j)]. To excite the flat-band states, the spots in the necklace are made with equal amplitude but alternating opposite phase [Fig. 3(c)], thus a localized "ring" mode is excited [Fig. 3(k)]. Lower insets in Figs. 3(b) and 3(c) show the interferograms of the input probe beams with a tilted quasi-plane wave, where we can clearly see the in-phase and out-of-phase relation between neighboring intensity spots of the probe beam through the interference fringes. More importantly, the interferogram [inset in Fig. 3(k)] taken at the output from the lattice reveals that the out-of-phase structure of the localized "ring" modes is preserved during propagation. Of course, these phase information can be better retrieved from the other technique such as that used in Ref. [28]. Clearly, the difference in performance between Figs. 3(j) and 3(k) emphasizes the relevance of the phase structure for the excitation of flat-band states. Based on the invariability of any linear combination of eigenmodes in the direction of propagation, we constitute a simple bound state [Fig. 3(d)] by the linear combination of two flat-band modes. Again, the nondestructive output pattern [Fig. 3(l)] is observed, indicating the feasibility for distortion-free image transmission based on arbitrary superposition of flat-band modes.

As compared with fs laser-written lattices [13, 14], the optically induced lattices have less propagation length due to the limitation of crystal length of 10 mm. It should be pointed that the propagation length in our experiment is about 1.2 coupling length (i.e., more than one coupling length). Furthermore, as shown in many prior experiments [2, 26], optically induced lattices (even only 10mm long) can allow for strong coupling between lattice waveguide channels. One can also see discrete diffraction from Fig. 3(i), indicating the coupling among waveguides. Thus, the localized patterns observed in Fig. 3 indeed arise from formation of flat-band modes rather than simple isolated wave-guiding. From numerical simulation, we found that the nearest-neighbor coupling constant is about 0.184 mm^{-1}, and the next nearest-neighbor coupling constant is about 0.014 mm^{-1}. Thus, the next-nearest-neighbor coupling is an order of magnitude smaller than the nearest-neighbor coupling, insignificant in our 10 mm-long lattices.

To further corroborate these experimental observations, we numerically solved the equation (1) by using the beam propagation method. The parameters are similar to those used in our experiments. $\lambda = 532$ nm, the lattice spacing $D = 28\mu$m, $n_0 = 2.35$, the index change associated with the induced Kagome lattices $\Delta n = 1.8 \times 10^{-4}$, and the propagation length $L = 10$mm corresponding to the experimental results. Typical results are shown in Fig. 4, where it can be clearly seen that our simulation results agree well with experimental results shown in Fig. 3. The first panel reveals the input probe beams, and the corresponding output patterns without lattices are shown in the middle panels. It can be seen that the input beams exhibit linear diffraction patterns without lattices. However, when the lattices are introduced, localization of the necklace-like beams is achieved as shown in the bottom panels. More importantly, the difference between distorted [Fig. 4(j)] and undistorted [Fig. 4(k)] is evident. This is in good agreement with previously performed numerical simulation [24]. In addition, we performed a series of simulations for different lattice constants and found that the localization was not ob-

#259832 Received 23 Feb 2016; revised 6 Apr 2016; accepted 11 Apr 2016; published 14 Apr 2016

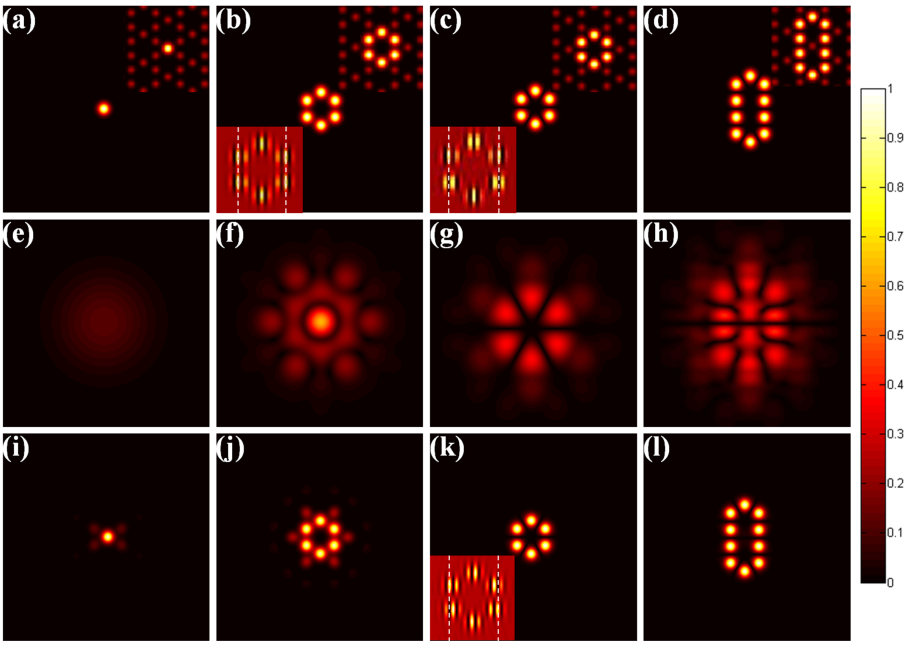

Fig. 4. Numerical simulation of localized flat-band states and their superposition through the Kagome lattices corresponding to Fig. 3. Other description is the same as for Fig. 3. $\lambda = 532$ nm, the lattice spacing $D = 28\mu$m, the index change associated with the induced Kagome lattices $\Delta n = 1.8 \times 10^{-4}$, and the propagation length $L = 10$ mm corresponding to the experimental results.

served after 10 mm propagation with the lattice spacing $D \leq 22\mu$m. This is because, when the lattice spacing is too small, strong coupling occurs even between the next-nearest neighbors, so the flat band can no longer preserve. Experimentally, we cannot achieve longer propagation distances due to the limitation of the crystal length. However, we have performed simulations to a longer propagation distance (60 mm), and we found that the diverse linear combinations of eigenmodes show little diffraction while propagating through the induced Kagome lattice [Fig. 5(a)].

In our experiments, weak disorder of the Kagome lattice (diagonal disorder) is present due to non-uniformity of light spot. Furthermore, we have performed linear-evolution simulations for flat-band mode transmission in Kagome lattices under random-noise perturbations. Figure 5 shows the numerical results. Upper row shows the output patterns of a single flat-band mode excited in the Kagome lattices under different random-noise perturbations. Lower row shows the corresponding linear-evolution simulations of long distance propagation. For a long distance propagation of 60 mm (about six coupling length), we have found that a flat-band "ring" state still remains robust and does not break up in the Kagome lattices with the random noise perturbations $d \leq 4\%$, as shown in Figs. 5(a) and 5(b). However, with 6% random noise perturbations, we can see some weak diffraction from the excited sites in Fig. 5(c). When the random noise perturbations reach to 10%, stronger diffraction can be seen and the "ring" mode is severely distorted [Fig. 5(d)]. Finally, we want to mention that in our simulation, we did not include the effect of anisotropic nonlinearity inherent in the biased photorefractive crystal. From the output lattice pattern [Fig. 2c] and also the discrete diffraction pattern of a Gaussian probe beam, we can see that, at the bias field we used, the anisotropic nonlinearity does not play an appreciable role here in deforming the Kagome lattice or its flat-band structure.

#259832 Received 23 Feb 2016; revised 6 Apr 2016; accepted 11 Apr 2016; published 14 Apr 2016

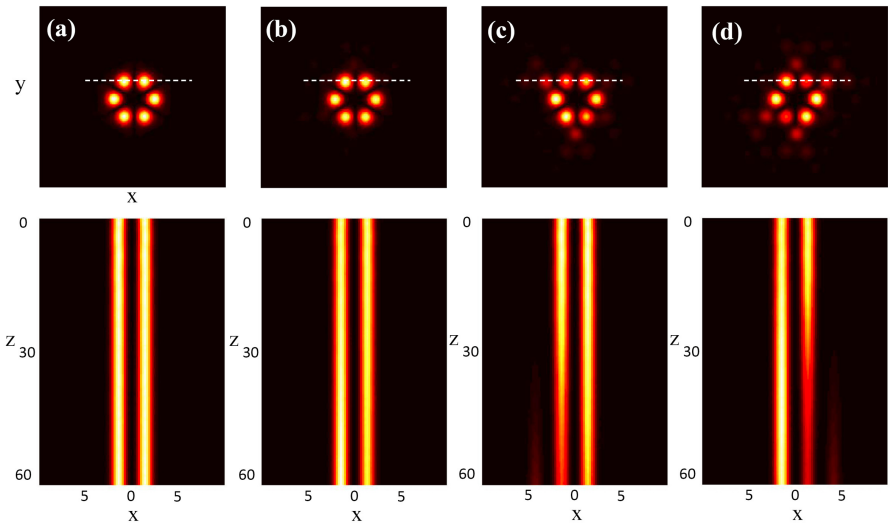

Fig. 5. Numerical simulation of long distance propagation (L=60mm) of localized flat-band states in Kagome lattices under random-noise perturbations. (a) random-noise perturbations $d = 0\%$; (b) $d = 4\%$; (c) $d = 6\%$; (d) $d = 10\%$. Upper row shows the output profiles of a single flat-band mode. Lower row shows the "sideview" evolution for mode profiles taken along the dashed line in top panels.

5. Conclusion

In conclusion, we have "fabricated" 2D Kagome photonic lattices in a bulk nonlinear crystal by optical induction and demonstrated experimentally the excitation of a flat-band state. Moreover, we have observed diffraction-free propagation of a complex pattern formed due to a superposition of the flat-band states in such Kagome lattices. These results further support the theoretical prediction of image transmission based on flat-band states in Kagome lattices [24]. Our work may provide inspiration for developing alternative light-trapping and image transmission schemes in structured photonic materials without engineered disorder or nonlinearity. In addition, one can envisage the possibility for experimental demonstration of predicted novel phenomena such as discrete flat-band solitons and PT-symmetric phase in Kagome photonic lattices [29, 30], Aharonov-Bohm photonic caging with the implementation of a synthetic gauge field [31].

Acknowledgment

This work was supported by the National Key Basic Research Program of China (2013CB632703, 2013CB328702), the National Science Foundation of China (NSFC) (11304165, 11504186, 61575098), and the 111 Project (B07013). We thank R. A. Vicencio for helpful discussion.

#259832 Received 23 Feb 2016; revised 6 Apr 2016; accepted 11 Apr 2016; published 14 Apr 2016